Proc. Natl. Acad. Sci. USA
Vol. 93, pp. 4827–4832, May 1996
Cell Biology

Sensitivity and selectivity of the DNA damage sensor responsible for activating p53-dependent G_1 arrest

LI-CHUN HUANG, KRISTIE C. CLARKIN, AND GEOFFREY M. WAHL*

Gene Expression Laboratory, The Salk Institute, 10010 North Torrey Pines Road, San Diego, CA 92037

Communicated by Mario R. Capecchi, University of Utah, Salt Lake City, UT, January 11, 1996 (received for review November 17, 1995)

ABSTRACT **The tumor suppressor p53 contributes to maintaining genome stability by inducing a cell cycle arrest or apoptosis in response to conditions that generate DNA damage. Nuclear injection of linearized plasmid DNA, circular DNA with a large gap, or single-stranded circular phagemid is sufficient to induce a p53-dependent arrest. Supercoiled and nicked plasmid DNA, and circular DNA with a small gap were ineffective. Titration experiments indicate that the arrest mechanism in normal human fibroblasts can be activated by very few double strand breaks, and only one may be sufficient. Polymerase chain reaction assays showed that end-joining activity is low in serum-arrested human fibroblasts, and that higher joining activity occurs as cells proceed through G_1 or into S phase. We propose that the exquisite sensitivity of the p53-dependent G_1 arrest is partly due to inefficient repair of certain types of DNA damage in early G_1.**

Normal cells evolve into cancers by a process of clonal evolution involving the accumulation of multiple genetic alterations. Many of these changes are initiated by chromosome breakage. Through induction of apoptosis or cell cycle arrest, a p53-dependent mechanism effectively prevents DNA damage present in G_1 from being replicated in S phase (1–6). As DNA breakage is likely to be the first step in the process of generating gene amplification, translocations, and deletions, it is understandable why cells with an intact p53 pathway do not produce descendants with such alterations at experimentally measurable rates (7–9). In contrast, inactivation of p53 alone allows immortalized nontumorigenic cells and primary fibroblasts to cycle in the presence of chromosome breaks and to undergo gene amplification at high rates (4, 10, 11). It is not surprising, therefore, that loss of p53 function is highly selected during cancer progression, and that defects in the p53 gene occur in more than 50% of human cancers (12).

The specific signals that induce p53-dependent G_1 arrest remain to be elucidated. Previous studies showed that ultraviolet light, ionizing radiation, and a variety of chemotherapeutic agents increase p53 levels (3, 4, 13, 14) and alter expression of p53 responsive genes (3, 15–17). However, in addition to DNA strand breaks, each of these perturbations induces cytoplasmic responses that may affect p53 concentration or modify its binding and transcription functions (18, 19). Therefore, the studies presented thus far may reflect contributions of both nuclear and cytoplasmic signals. One study (20) concluded that DNA damage is sufficient to increase p53 levels because electroporation of active restriction enzymes induced p53 to a higher level than electroporation of inactive restriction enzymes in a myeloid leukemia cell line. However, this conclusion is compromised by the observation that procedures such as calcium phosphate treatment can induce p53 in other cells (21). Furthermore, because subtle treatments that do not elevate p53 content can activate p53 function and induce the expression of p53 target genes (22), it is possible that the arrest response could be triggered in the absence of a measurable increase in p53 level. In addition, if DNA damage is the trigger, it is unclear whether DNA damage other than double strand breaks, such as single-stranded gaps, provokes the arrest response. The latter is important given increasing evidence of p53 involvement in nucleotide excision repair (17, 23). Furthermore, the number of damaged sites that activate the arrest mechanism has not been determined since the strategies employed thus far are incapable of producing a defined number and type of lesions. The answers to these questions are vital for understanding how p53 prevents the development of chromosome changes such as gene amplification that could be initiated by a solitary double strand break (24).

We utilized nuclear microinjection of defined DNA substrates to assess the specific contributions of different types of DNA damage to p53-mediated arrest and to quantify the sensitivity of the arrest mechanism. We show that supercoiled or nicked plasmid DNA did not affect cell cycle progression. Linearized plasmid DNA with any of several terminal configurations and single-stranded phagemid DNA induced a p53-dependent G_1 arrest. Results obtained after serial dilution of linearized DNA are consistent with the proposal that a solitary double strand break is sufficient to induce G_1 arrest. Polymerase chain reaction (PCR) assays showed that end-joining activity was low in serum-arrested normal fibroblasts, and higher joining activities were detected as cells proceeded through G_1 or into S phase. Since gene amplification could arise from just one DNA break, we propose that the exquisite sensitivity of the p53-dependent G_1 arrest, partly due to inefficient repair of double strand breaks, explains the effectiveness with which this mechanism prevents proliferation of cells with structural chromosome changes.

MATERIALS AND METHODS

Cell Culture. WS1 human embryonic skin fibroblast, obtained from the American Type Culture Collection (CRL 1502), was cultured for no longer than eight passages in Dulbecco's modified Eagle's medium (DMEM) supplemented with 10% fetal bovine serum (FBS). WS1E6 was constructed by infecting WS1 with a retroviral vector that expresses the E6 protein from human papilloma virus 16 (25). WS1E6 cells were also maintained in DMEM supplemented with 10% FBS and 400 μg of active Geneticin per ml (G418; GIBCO). GM47.23 was cultured in Earle's minimal essential medium (MEM) with 10% FBS in a humidified atmosphere containing 7% CO_2/93% air at 37°C as described by Yin *et al.* (11). Cells were arrested in G_0 by incubating them for 40–52 h in DMEM with 0.1% serum. They were stimulated to reenter the cell cycle by adding 20% FBS. Cell cycle progression was monitored by measuring bromodeoxyuridine (BrdUrd) incorporation (see below).

DNA Substrates. The plasmid DNA substrates were prepared as follows. Supercoiled Bluescript KSII$^+$ DNA (pBSKSII$^+$; Stratagene) was purified using Qiagen (Chatsworth, CA)

The publication costs of this article were defrayed in part by page charge payment. This article must therefore be hereby marked "*advertisement*" in accordance with 18 U.S.C. §1734 solely to indicate this fact.

Abbreviations: FITC, fluorescein isothiocyanate; Dex, dexamethasone, BrdUrd, 5-bromodeoxyuridine.

*To whom reprint requests should be addressed.

columns following the procedure recommended by the manufacturer. Restriction endonuclease digestions were as recommended by the manufacturers (New England Biolabs or Stratagene). Nicked plasmid DNA was prepared by DNase I treatment in the presence of 150 μg of ethidium bromide per ml according to Shibata *et al.* (26), and the product was identified and purified by gel electrophoresis. Single-stranded circular Bluescript DNA was prepared from a phage preparation using the helper phage R408 (Stratagene). Phage particles were grown as described (27) and purified from CsCl gradients and extracted with phenol. The single-stranded circular DNA was further purified by gel electrophoresis by using low-melting agarose followed by β agarase treatment (New England Biolabs). The 2.9-kb gapped circle was prepared by annealing excess amounts of an oligo (5′-AGCCTGGGGT-GCCTAAT-3′) to the single-stranded circular phagemid. This was done by mixing the oligo and the single-stranded circular molecules and incubating at 90°C for 10 min, followed by slow cooling to room temperature. A Sephadex G50 column was used to remove excess primers. The gapped duplex form was confirmed by digestion with *Ban*I, which cleaves within the double-stranded region. The 25-nt gapped duplex was generated by recA-mediated strand exchange reactions (28). The reactions were carried out using *Eco*RV and *Bam*HI linearized pBSKSII$^+$ and single-stranded circular phagemid DNA as the substrates. The product was identified and purified by gel electrophoresis. Double-stranded oligonucleotides were made by annealing complementary single-stranded oligonucleotides, and then purified over Sephadex G50 column to remove single-stranded material. All DNA was purified by phenol/chloroform (1:1; vol/vol) extraction and ethanol precipitation. The concentration of the DNA was determined by OD_{260}.

Microinjections and Cell Cycle Analyses. Microinjections were done using a semiautomatic micromanipulator/injector (Eppendorf micromanipulator 5172 and microinjector 5242) with needles pulled from glass capillaries on a horizontal pipette puller (Narishige, Tokyo). Plasmid Bluescript KSII$^+$ DNA was injected at a concentration of 5 ng/μl unless indicated otherwise. After injection, cells were placed in media containing 20% FBS and 10 μM 5-bromodeoxyuridine (BrdUrd) for 24 h. The fixation and staining procedures were the same as described by La Morte *et al.* (29). The results were scored and photographed with a Zeiss fluorescence microscope (standard WUL) using identical exposure times for each filter. The fluorescent fields were photographed with Kodak Ektachrome film (ASA400) under ×63 objective. The injected DNA was later analyzed to determine the repair activity at various stages in the cell cycle. Normal human diploid fibroblasts were synchronized in G_0/G_1 by serum deprivation before microinjection and then released into serum containing medium along with BrdUrd to monitor their capacity to progress into S phase. The efficiency of S phase entry of the injected cells was compared with that of adjacent cells that were not injected with DNA.

Cell Lysates and PCRs. To extract total DNA from injected cells for PCR, cells were washed once with PBS and incubated overnight at 60°C in lysis buffer containing 10 mM Tris·HCl (pH 7.5), 10 mM EDTA, 10 mM NaCl, 0.5% Sarcosyl, and 1 μg of Proteinase K per ml. The total DNA lysate was collected, precipitated with 0.3 M sodium acetate and 2.5 × volume ethanol, and resuspended in 30 μl buffer containing 10 mM Tris·HCl and 1 mM EDTA (pH 7.5).

Oligo primers were synthesized using MilliGen/Biosearch cyclone plus DNA synthesizer. The primer set used for amplification of internal plasmid sequence is 5′-AGCGAG-GAAGCGGAAGA-3′ and 5′-AGCCTGGGGTGCCTAAT-3′. Two sets of primers were used to amplify junction plasmid sequence: (*i*) the M13–20 and reverse primers from Stratagene (5′-GTAAAACGACGGCCAGT-3′ and 5′-AACAGCTGA-CCATG-3′) and (*ii*) the primers 5′-GGGTTTTCCCAGTC-ACGA-3′ and 5′-GCACCCCAGGCTTTACAC-3′. PCRs were carried out using Boehringer Mannheim buffer, 2.5 units of *Taq* polymerase, and 10 μl cell lysate in a total volume of 100 μl. Cycle conditions were as follows: denaturation at 90°C for 1 min, annealing at 55°C for 1 min, and extension at 72°C for 1 min for a total of 30 cycles using an Ericomp thermocycler.

RESULTS AND DISCUSSION

Experimental Design. Previous studies showed that irradiation of normal human diploid fibroblasts prior to the G_1 restriction point induced a p53-dependent arrest (3). The magnitude of induction of p53 and p53 target genes and of G_1 arrest were identical after irradiating normal human diploid fibroblasts synchronized by serum depletion, serum depletion followed by release for up to 12 h (3), or after synchronization by confluence (30). Therefore, for experimental convenience, we analyzed the effects on G_1 progression by injecting DNA into nuclei of normal human diploid fibroblasts synchronized in G_0/G_1 by serum deprivation. *In vitro* modified Bluescript II$^+$ plasmid (pBSKSII$^+$) was injected unless noted otherwise. Injected cells were marked by coinjection of rabbit IgG. Immediately after injection, the cells were incubated in medium containing 20% FBS and 10 μM BrdUrd for 24 h, and then fixed, stained with fluorescein isothiocyanate (FITC)-labeled antibodies against rabbit IgG and biotinylated antibodies against BrdUrd (detected with Texas Red conjugated streptavidin), and counterstained with Hoechst 33258. Fluorescence microscopy reveals blue uninjected cells resulting from the Hoechst counterstain, or red if they entered S phase. Injected cells that arrested were blue-green because of the additional FITC signal. Finally, injected cells that cycled into S phase showed the Texas Red signal indicative of BrdUrd incorporation. Typical fluorescence micrographs of injected WS1 normal human diploid fibroblasts are shown in Fig. 1. The data are presented as the percentage of BrdUrd$^+$ injected cells relative to the percentage of BrdUrd$^+$ uninjected surrounding cells.

G_1 Arrest Is Induced by Nuclear Injection of Various DNA Substrates. Nuclear injection of linearized pBSKSII$^+$ arrested normal human diploid fibroblasts. Fig. 2 summarizes the results normalized against uninjected controls. While 20–50% of uninjected cells entered S phase within the 24-h release period, only 2–7% of the cells injected with linearized DNA underwent DNA synthesis. Plasmid DNA linearized by restriction enzymes that produced blunt ends, 5′ overhangs, 3′ overhangs, or two different noncomplementary termini on

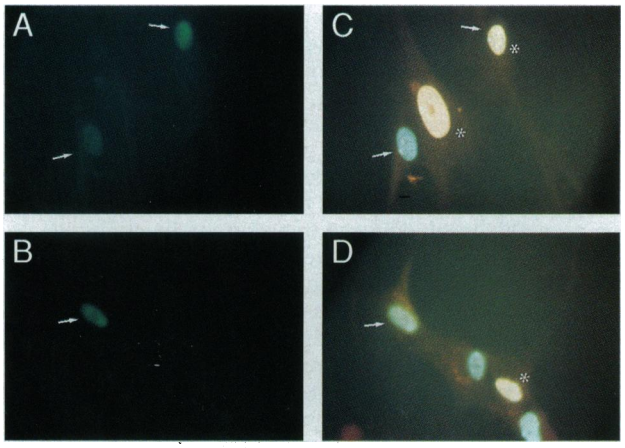

FIG. 1. Example of immunofluorescence staining of injected cells. (*A* and *B*) FITC stained (green, injected) nuclei. (*C* and *D*) Texas red stained (red, S phase) and Hoechst dye stained (blue, G_1) nuclei. Supercoiled pBSKSII$^+$ DNA (*A* and *C*) or *Eco*RV-linearized pBSKSII$^+$ DNA (*B* and *D*) at 5 ng/μl (≈100 molecules per nucleus) was injected. Arrows indicate the positions of the injected nuclei. Asterisks indicate BrdUrd$^+$ nuclei stained with Texas red. See text for additional description.

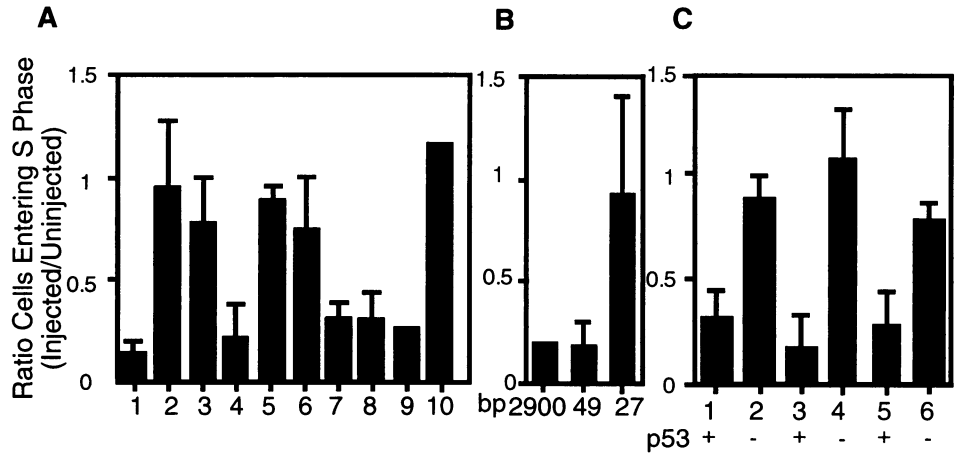

FIG. 2. p53-dependent cell cycle arrest by nuclear injections. (*A*) Effect of injecting various forms of Bluescript KSII$^+$ DNA on cell cycle progression. The numbers below each bar represent the treatment listed below. All injections were nuclear, except 10 (cytoplasmic), and used Bluescript KSII$^+$ DNA except where noted. Bars: 1, uninjected cells kept in serum starvation medium; 2, nuclear injection of buffer alone; 3, supercoiled; 4, *Eco*RV linearized; 5, nicked; 6, circular duplex containing a 25-nt gap; 7, circular duplex containing a 2.9-kb gap; 8, single-stranded circular; 9, supercoiled plus *Eco*RV linearized DNA; 10, *Eco*RV linearized DNA (cytoplasmic injeciton). The DNA concentration was 5 ng/μl, except in bar 9 where 0.6 ng/μl *Eco*RV linearized DNA and 6 ng/μl supercoiled DNA were injected. Fifty to 150 injected nuclei were scored for each experimental point. The results of three independent experiments are presented by the mean ($\pm$SD) of the ratio of the percentage of injected cells that underwent DNA synthesis to the percentage of uninjected surrounding cells that underwent DNA synthesis. The fraction of cells entering S phase in serum starvation medium is also shown for comparison. Supercoiled plus linear DNA (bar 9) is a single experiment scored from 108 injected nuclei. Cytoplasmic injection of linearized DNA (bar 10) is also a single experiment scored from 78 injected cells. (*B*) Effect of injecting various lengths of double-stranded linear DNA on cell cycle progression. DNA molecules were injected at 1000 molecules per cell. The results of three independent experiments are presented by the mean ($\pm$SD) of the ratio of the percentage of injected cells that underwent DNA synthesis to the percentage of uninjected surrounding cells that underwent DNA synthesis. The double-stranded 27 mer is a blunt-ended molecule with the sequence 5′-GATATGTAGGGATAACAGGGTAATGAT-3′. The double-stranded 49 mer is annealed by 5′-GATCCATAACTTCGTATAG-CATACATTATACGAAGTTATTTAATTAAGC-3′ and 5′-GGCCGCTTAATTAAATAACTTCGTATAATGTATGCTATACGAAGTT-ATG-3′. (*C*) Arrest induced by linearized plasmid DNA or single-stranded circular DNA is p53 dependent. Bars: 1, WS1 cells injected with single-stranded circular DNA; 2, WS1E6 cells injected with single-stranded circular DNA; 3, WS1 cells injected with *Eco*RV linearized plasmid DNA; 4, WS1E6 cells injected with *Eco*RV linearized plasmid DNA; 5, GM47.23 injected with *Eco*RV linearized plasmid DNA, released with 0.5 mM Dex; and 6, GM47.23 injected with *Eco*RV linearized plasmid DNA, released without Dex. DNA was at a concentration of 5 ng/μl. The mean ($\pm$SD) of the ratio of the percentage of injected cells that underwent DNA synthesis to the percentage of uninjected surrounding cells that underwent DNA synthesis was calculated for three independent experiments and is shown here. s.s.c., Single-stranded circular; d.s., double stranded.

individual molecules were equally effective in arresting cells (data not shown). The arrest signal is not generated by mechanical injury as nuclear injection of supercoiled plasmid, nicked circular DNA, buffer alone, or cytoplasmic injection of linearized plasmid DNA failed to arrest normal human diploid fibroblasts (Fig. 2*A*). There is a length threshold for activating the arrest mechanism as 49-bp, but not 27-bp duplex oligonucleotides, induced arrest (Fig. 2*B*). However, 49-bp duplexes were not as effective as 2.9-kb linear plasmids when injected at low concentrations (data not shown). There is an apparent specificity to the damage sensor as single-stranded circular phagemid DNA also induced an arrest, while nicked plasmid DNA, and short, single-stranded molecules, such as 17- to 49-nt oligonucleotides, did not have a significant effect (Fig. 2*A* and data not shown). Taken together, these data demonstrate that nuclear DNA damage alone is sufficient to induce an arrest, and that the damage does not have to be generated within host chromosomes.

The plasmid, single-stranded phagemid, and double-stranded 49 mer used in this study did not contain a eukaryotic promoter, so it is unlikely that components of the transcription machinery, such as transcription factor TFIIH (31, 32), are required in the sensing mechanism. However, nuclear accumulation of p53 has been reported to result from transcription inhibition (33). While nuclear accumulation of p53 has often been correlated with arrest induction (3, 14), the arrest response may not depend on increasing p53 concentration. This is supported by recent data that activation of the DNA binding and transcriptional activation function of p53 can be achieved by converting inactive to active tetramers by binding of specific peptides or antibodies (22). Consistent with the model of p53 activation by posttranslational modification, we did not observe an increase in p53 level in the majority of cells arrested by linearized DNA using an immunofluorescence assay (data not shown).

Arrest Induced by Microinjection Requires Functional p53. We determined whether p53 function is required for cell cycle arrest by injecting linearized plasmid or single stranded phagemid into normal human diploid fibroblasts expressing the E6 gene cloned from an oncogenic human papillomavirus (i.e., WS1E6). WS1E6 fibroblasts express no detectable p53 protein and do not arrest when γ-irradiated (25). Nuclear injection of hundreds of linearized or single-stranded pBSKSII$^+$ molecules failed to arrest WS1-E6 in G_1 (Fig. 2*C*). Furthermore, linearized plasmid DNA induced a G_1 arrest in a glioblastoma cell line, GM47.23, expressing a dexamethasone (Dex) inducible wild-type p53 gene (Fig. 2*C*) (11, 34), but only after p53 induction by Dex treatment. Thus, cell cycle progression of fibroblasts and epithelial derived tumor cells was significantly affected by injection of linearized plasmid DNA only when wild-type p53 protein was present.

Estimating the Amount of Damage Required to Activate the Sensor. We estimated the minimum number of molecules required to arrest normal human diploid fibroblasts by injecting serially diluted, double-stranded linearized DNA (Fig. 3*A*). The approximate number of molecules injected was estimated by assuming that the maximal injected volume is equivalent to 0.1 nuclear volume ($\approx 10^{-13}$ liter) (35). Injecting a maximum of 1.5 molecules per cell produced a small but reproducible decrease in the number of cells capable of entering S phase relative to controls in which buffer or supercoiled DNA was introduced. By contrast, injecting 15 or fewer molecules per nucleus reduced the number of cells entering S phase to that observed in the serum-arrested control. The fraction of arrested cells was not increased by injecting up to 150 molecules per cell.

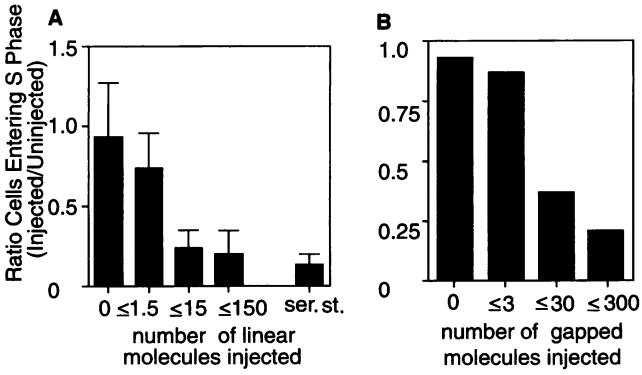

FIG. 3. Small amounts of DNA damage induce G_1 arrest. (*A*) Effect of linearized plasmid DNA. WS1 cells were injected with *Eco*RV linearized pBSKSII$^+$ DNA at concentrations of 0, 50 pg/μl, 500 pg/μl, or 5 ng/μl. The maximal number of molecules injected per nucleus is indicated. The results from three independent experiments and 70–150 nuclei were scored for each analysis. ser. st., Serum starved. (*B*) Effect of primed, single-stranded circular DNA. WS1 cells were injected with primed single-stranded circular phagemid pBSKSII$^+$ DNA at concentrations of 0, 50 pg/μl, 500 pg/μl, or 5 ng/μl. The estimated maximal number of molecules injected per nucleus is indicated. Fifty to 200 nuclei were scored for each concentration.

The data obtained from the microinjection approach indicates that very few broken ends induce a p53-dependent G_1 arrest. However, the precise number of broken ends required to induce arrest is difficult to determine accurately using the microinjection paradigm we employed because the actual injection volume successfully delivered into individual nuclei may vary by a factor of 5 or more (36). We are quite certain that most injections delivered far less than 0.1 nuclear volume because injecting larger volumes is cytotoxic, and because all of the injected volume may not be retained in the nucleus. Other data suggest that the average injection volume may be only 0.01–0.02 nuclear volume (37). The data in Fig. 3 are presented to reflect experimental uncertainties by showing the maximum number of molecules we expected to be delivered using DNA solutions of precisely known concentration. It is most likely that many cells injected with a maximum of 1.5 molecules per nucleus would not have received any DNA, which is consistent with the ability of almost all of the cells injected at this concentration to enter S phase. By the same reasoning, the majority of cells injected with a maximum of 15 linear molecules should have received at least one broken end. Fig. 3 shows that the fraction of cells that arrested after injecting 15 or fewer molecules per nucleus was the same as observed in the serum-arrested control. Thus, the maximum arrest was observed under conditions when all injected cells received at least one broken DNA molecule. Data from two additional independent approaches suggest that a single unrepaired or irreparable lesion may be sufficient to activate the G_1 arrest response in human and rodent cells. First, a dose kinetic analysis of G_1 arrest after gamma-radiation exhibited single-hit kinetics in the same normal human diploid fibroblast strain used for the current studies (3). Second, breakage of a single dicentric chromosome in a cell expressing wild-type p53 induced a prolonged G_1 arrest (38). Taken together, the results of these three experimental approaches lead us to propose that one double-stranded break is sufficient to induce a p53-dependent G_1 arrest in the cell types analyzed.

DNA End-Joining Efficiency During the Cell Cycle. Eukaryotic cells can repair many of the types of DNA damage that we found led to p53-dependent G_1 arrest (39, 40). However, two independent experimental approaches indicated that repair capacity was reduced or absent in serum-starved normal human diploid fibroblasts. First, we determined whether cells in G_0/G_1 are arrested by gapped circular DNAs. A circular substrate with a large gap made by priming single-stranded phagemid DNA arrested cells in G_1 (Fig. 2*A*), though the arrest potential appeared to be slightly less than that of linearized double-stranded molecules (Fig. 3). By contrast, a substrate with a 25-nt gap failed to induce arrest (Fig. 2*A*). Assuming an elongation rate of 3 kb/min (41), it would take approximately 1 min to fill the 2.9-kb gap present in the substrate containing a 17-nt primer. The data suggest that serum-arrested cells do not efficiently fill in long gaps to create products that do not induce arrest. However, either short gaps can be filled in sufficiently rapidly to avoid triggering the arrest response, or the 25-nt gap was of insufficient length to trigger the arrest response.

We next investigated whether serum-starved normal human diploid fibroblasts could join the ends of double strand breaks. We reasoned that joining the ends of linearized substrates to form covalently closed or nicked circular DNA would generate molecules incapable of arresting cells. We first sought to determine if the double strand break in the injected plasmid molecules could be repaired if an intact circular homologue was provided. The experiment was based on the observation that the repair of double strand breaks in yeast is frequently mediated by recombination with the homologous chromosome or sister chromatid (42). Coinjection of supercoiled and linearized plasmid DNA into serum-starved WS1 nuclei blocked cell cycle progression as effectively as linearized plasmid DNA alone (Fig. 2*A*). This result shows that the arrest potential of double strand breaks is not diminished by intact homologous sequences in G_0/G_1 cells.

A PCR strategy was next used to monitor directly the capacity of normal human diploid fibroblasts to join broken ends. G_0/G_1 arrested cells did not efficiently degrade injected DNA (Fig. 4*B*), suggesting that these cells have low levels of the exonuclease activities previously reported to be involved in repair and recombination events (43). On the other hand, little or no product was obtained when primers positioned on either side of the double strand break were used for amplification (Fig. 4*B*). Occasionally a small amount of product was detected, but it probably was generated by end-joining activity present in the small fraction of cells that progressed into S phase during serum arrest (ref. 3 and see below). The results indicate that very few, if any, of the blunt ends of the injected DNA were joined in G_0 arrested cells.

Previous studies showed that radiation failed to arrest normal human diploid fibroblasts that progressed to or beyond the G_1 restriction point (3). Since p53 overexpression results in transcriptional activation of downstream effectors such as p21 in G_2/M (44), it is unlikely that loss of p53 transcription activation capacity contributed to the inability to induce an arrest beyond the restriction point. One factor that could contribute to reduced capacity for arrest would be an increased capacity to join broken ends, resulting in elimination of the required signal. Consistent with this proposal, the time course analysis shown in Fig. 4*C* reveals that normal human diploid fibroblasts regain joining activity as they progress into G_1. A small amount of product of the size expected for end-joining was detected when serum-arrested cells were released into serum for 3 h, injected, and then harvested 2-h later. A smaller aberrant product was observed, but it reflects amplification in the absence of end-joining as it was also observed when linearized DNA was amplified *in vitro*. The amount of *bona fide* end-joining product increased in cells released into serum for 7 and 16 h before injection (Fig. 4*C*, lanes 2 and 3). The predominant, reproducible product exhibited the size expected for head-to-tail joining, although tail-to-tail and head-to-head products were generated at lower efficiencies. All valid end-joining products hybridized to an oligonucleotide specific for the junction region (data not shown). The joining patterns observed at 7 and 16 h after release were similar to those observed for plasmid recombination in asynchronous human cells (45). As human cells release from serum synchronization and enter S phase at very different rates (46), it is not possible to state whether

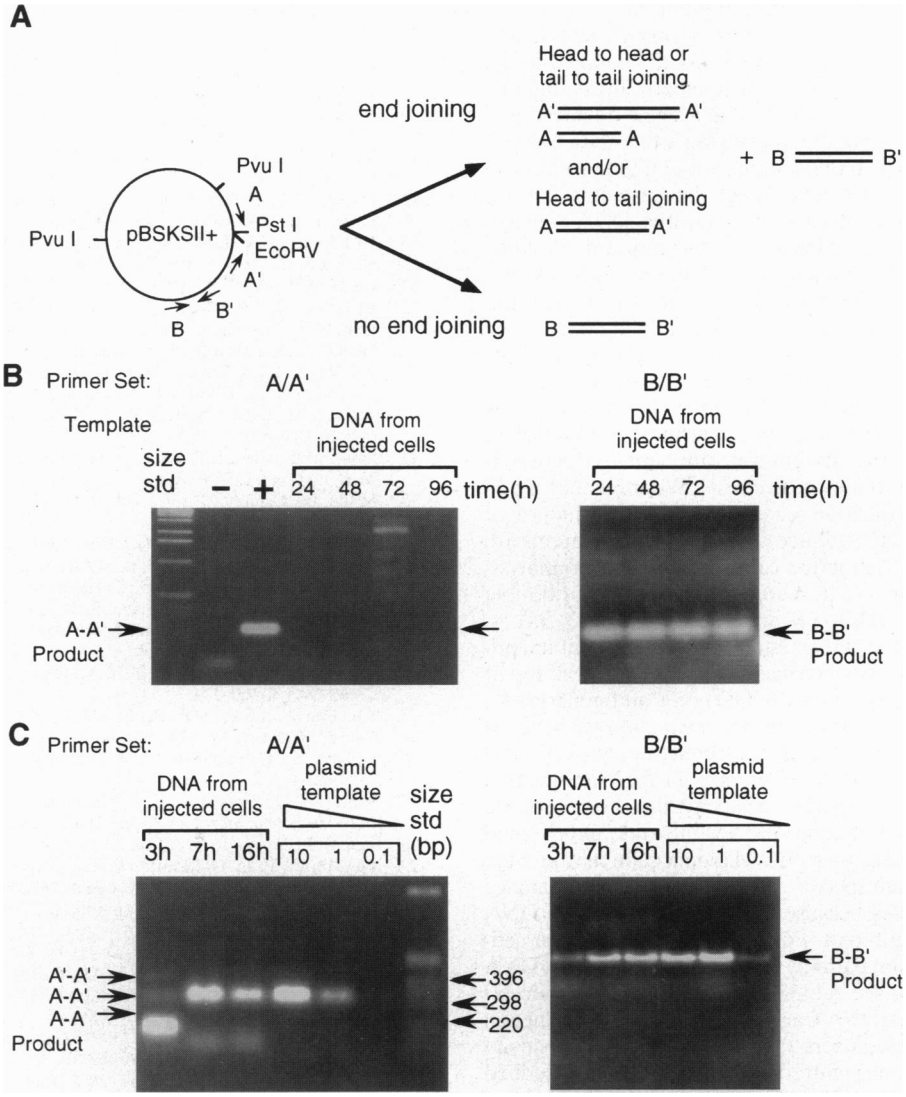

FIG. 4. PCR detection of end-joining activity. (*A*) Experimental strategy and map of pBSKSII$^+$ showing the primers used in PCR detection of junction and internal sequences. Plasmid restricted with the indicated enzymes was injected at about 1000 molecules/cell. Total DNA was isolated at the indicated times and subjected to PCR using primers flanking the cleavage site, or as a positive control, in an uncut region adjacent to the cleavage site. Joining is indicated by formation of PCR products using the A-A′ primers. The *Eco*RV and *Pst*I sites used in this study are located in the multiple cloning site region of the pBSKSII$^+$ plasmid. Primers A–A′, junction primers; primers B–B′, internal primers. Two sets of junction primers were used in the study. The expected size of the internal product is 159 bp. The distance between the internal primer B′ and the *Eco*RV/*Pst*I restriction sites is approximately 200 bp. (*B*) Results of injecting linearized DNA into serum-arrested cells. About 100 ng/μl of *Eco*RV linearized plasmid DNA was injected during serum starvation followed by release of cells into complete medium containing 20% FBS. It was estimated that at least 1 pg of the injected DNA was used in amplification (19). (*Left*) PCR amplification using primers (M13–20 and reverse) specific for the junction sequences. These primers produced a PCR junction product of 224 bp. +, Positive control using 1 pg of *Pvu*I linearized pBSKSII$^+$ DNA for PCR amplification. A single band of the expected size (224 bp) was obtained. −, Negative control; junction product was not produced when *Eco*RV linearized pBSKSII$^+$ DNA was used in reaction. PCR amplification of DNA isolated from each time point produced barely detectable levels of the unique junction product. (*Right*) PCR amplification using primers (B–B′) specific for internal sequences. A single band of the expected size (159 bp) and of approximately equal intensity was amplified at each time point. The size standard used in both panels is 1-kb ladder (BRL). (*C*) PCR product from cells injected with *Pst*I linearized pBSKSII$^+$ DNA. (*Left*) PCR product using junction primers 5′-GGGTTTTCCCAGTCACGA-3′ and 5′-GCACCCCAGGCTTTACAC-3′. (*Right*) Product from internal primers; head-to-tail end-joining of *Pst*I linearized pBSKSII$^+$ DNA will produce a PCR product with a size of 324 bp, and head-to-head or tail-to-tail joining, 402 bp or 246 bp. After serum release, cells were injected with 100 ng/μl *Pst*I linearized pBSKSII$^+$ DNA at the indicated times and DNA was isolated 2 h after injection. In lane 3h, the prominent smaller band (about 200 bp) is an aberrant PCR product from amplifying *Pst*I linearized pBSKSII$^+$ DNA. All DNA was linearized with *Pvu*I before PCR. The plasmid template used in the positive controls was *Pvu*I digested pBSKSII$^+$. The amounts of template DNA were 10, 1, and 0.1 pg. The size standard shown on the left is a 1-kb ladder.

the joining activity was acquired in G_1 cells, or only after they entered S phase.

The limited ability of G_0/G_1 arrested normal human diploid fibroblasts to join double strand breaks by direct end joining or recombinational repair, along with other data showing long-term arrest in response to γ-radiation, are inconsistent with the proposal that wild-type p53 induces a transient G_1 arrest to allow for repair of double strand breaks and other types of DNA damage (4). Although more general conclusions regarding the fate of damaged DNA in G_1 arrested cells await analyses of other types of DNA repair, the data presented here and elsewhere (3) lead us to propose that p53 maintains genomic stability by removing cells from the cycle if breakage occurs in G_0 or before the G_1 restriction point (3). If breakage occurs after the restriction point, and repair produces a dicentric chromosome, breakage of this structure in anaphase would be sufficient to trigger an arrest in the following G_1. Detection of broken chromosomes by the p53-dependent arrest mechanism described here would result in

the continuous elimination of cells containing just one broken chromosome. In addition, if telomeres of insufficient length appear as double strand breaks, then p53 could be linked to the senescence clock proposed to be set by telomere shortening (47, 48). While some experiments indicate that a single double strand break induces lethality in budding yeast (49), other data indicate that a solitary double strand break induces a transient arrest (50). As a p53 homologue has not been detected in yeast thus far, it is possible that metazoans evolved a more sensitive DNA damage-activated arrest mechanism to insure effective removal of mitotic cells entering the cycle with a single break in any chromosome.

The components of the nuclear damage sensor are unknown. *In vitro* data are compatible with p53 being part of the sensor as it reanneals single-stranded DNA (51), and its sequence-specific DNA binding is activated by single stranded oligonucleotides shorter than ≈40 nt (52). Importantly, our data demonstrate that the types of substrates that stimulate purified p53 to recognize its binding site are ineffective at triggering G_1 arrest in tissue culture cells. We infer that if p53 participates directly in damage recognition and transduction of the appropriate signals to produce G_1 arrest, other proteins are likely to be involved. Attractive candidates awaiting analysis include proteins implicated in recognition or repair of double strand breaks, such as DNA-PK and Ku antigens (53, 54).

Our observation that serum-arrested cells are deficient in end-joining capacity was unexpected since double strand break repair capacity in Chinese hamster ovary (CHO) cells and nonhomologous end-joining activity measured by transformation efficiency of Rat20 cells by linearized plasmid were detected throughout the cell cycle (55, 56). However, many differences in the experimental system, such as p53 status, species specificity, tissue origin of the cell types employed, and method of detecting end joining could contribute to apparent discrepancies. Microinjection may provide a unique way to elucidate specific contributions of DNA damage alone to repair processes because conditions that induce DNA damage may also affect repair. For instance, UV radiation activates a signal transduction pathway resulting in unscheduled DNA synthesis (for a review, see ref. 57). By contrast, direct nuclear microinjection of broken DNA fragments should bypass induction of cytoplasmic signal transducers and result in maximal sensitivity to the types of DNA damage introduced. The approach described here also provides a tractable system for exploring the precise DNA structures sensed *in vivo* by the arrest machinery. It should also facilitate identifying the factors involved in transducing signals from damaged DNA to the cell cycle control machinery, for repairing various types of DNA damage, and for inducing the DNA repair machinery in noncycling cells.

This paper is dedicated to the memory of Mr. Pao-hsiang Huang for his lifelong support and encouragement of his daughter. We thank Drs. J. Meinkoth and V. La Morte and Ms. D. E. Wofford for technical assistance with microinjection; S. Linke for WS1E6 cells; L. Iype and W. Bedale for the recA protein and DNA purification protocols, Dr. M. I. Aladjem for the 27 mer and 49 mer double-stranded oligonucleotides, and Drs. J. Feramisco, S. O'Gorman, R. E. Kelly, and M. I. Aladjem and Ms. L.L. Brody for discussion and comments on the manuscript. We thank the M. Chris Dixon Foundation for supporting the purchase of the microinjector. L.-c.H. was supported by the Charles H. and Anna S. Stern Foundation. This work was supported by grants from the National Cancer Institute to G.M.W. and by the G. Harold and Leila Y. Mathers Charitable Foundation.

1. Clarke, A. R., Purdie, C. A., Harrison, D. J., Morris, R. G., Bird, C. C., Hooper, M. L. & Wyllie, A. H. (1993) *Nature (London)* **362,** 849–852.
2. Lane, D. P. (1992) *Nature (London)* **358,** 15–6.
3. Di Leonardo, A., Linke, S. P., Clarkin, K. & Wahl, G. M. (1994) *Genes Dev.* **8,** 2540–2551.
4. Kastan, M. B., Onyekwere, O., Sidransky, D., Vogelstein, B. & Craig, R. W. (1991) *Cancer Res.* **51,** 6304–6311.
5. Lowe, S. W., Schmitt, E. M., Smith, S. W., Osborne, B. A. & Jacks, T. (1993) *Nature (London)* **362,** 847–849.
6. Lowe, S. W., Ruley, H. E., Jacks, T. & Housman, D. E. (1993) *Cell* **74,** 957–967.
7. Tlsty, T. D., Margolin, B. H. & Lum, K. (1989) *Proc. Natl. Acad. Sci. USA* **86,** 9441–9445.
8. Tlsty, T. D. (1990) *Proc. Natl. Acad. Sci. USA* **87,** 3132–3136.
9. Wright, J. A., Smith, H. S., Watt, F. M., Hancock, M. C., Hudson, D. L. & Stark, G. R. (1990) *Proc. Natl. Acad. Sci. USA* **87,** 1791–1795.
10. Livingstone, L. R., White, A., Sprouse, J., Livanos, E., Jacks, T. & Tlsty, T. D. (1992) *Cell* **70,** 923–935.
11. Yin, Y., Tainsky, M. A., Bischoff, F. Z., Strong, L. C. & Wahl, G. M. (1992) *Cell* **70,** 937–948.
12. Harris, C. C. (1993) in *Accomplishments in Cancer Research 1992*, eds. Fortner, J. G. & Rhoads, J. E. (Lippincott, Philadelphia), pp. 179–188.
13. Di Leonardo, A., Linke, S. P., Yin, Y. & Wahl, G. M. (1993) *Cold Spring Harbor Symp. Qaunt. Biol.* **58,** 655–667.
14. Lu, X. & Lane, D. P. (1993) *Cell* **75,** 765–778.
15. El-Deiry, W. S., Harper, J. W., O'Connor, P. M., Velculescu, V. E., Canman, C. E., Jackman, J., Pietenpol, J. A., Burrell, M., Hill, D. E., Wang, Y., Wiman, K. G., Mercer, W. E., Kastan, M. B., Kohn, K. W., Elledge, S. J., Kinzler, K. W. & Vogelstein, B. (1994) *Cancer Res.* **54,** 1169–1174.
16. El-Deiry, W. S., Tokino, T., Velculescu, V. E., Levy, D. B., Parsons, R., Trent, J. M., Lin, D., Mercer, W. E., Kinzler, K. W. & Vogelstein, B. (1993) *Cell* **75,** 817–825.
17. Smith, M. L., Chen, I. T., Zhan, Q., Bae, I., Chen, C. Y., Gilmer, T. M., Kastan, M. B., O'Connor, P. M. & Fornace, A. J. (1994) *Science* **266,** 1376–1380.
18. Milne, D., Campbell, L., Campbell, D. & Meek, D. (1995) *J. Biol. Chem.* **270,** 5511–5518.
19. Wu, H. & Lozano, G. (1994) *J. Biol. Chem.* **269,** 20067–20074.
20. Nelson, W. G. & Kastan, M. B. (1994) *Mol. Cell. Biol.* **14,** 1815–1823.
21. Renzing, J. & Lane, D.(1995) *Oncogene* **10,** 1865–1868.
22. Hupp, T. R., Sparks, A. & Lane, D. P. (1995) *Cell* **83,** 237–246.
23. Smith M. L., Chen I. T., Zhan Q., O'Connor P. M. & Fornace A. J. (1995) *Oncogene* **10,** 1053–1059.
24. Windle, B., Draper, B. W., Yin, Y. X., O'Gorman, S. & Wahl, G. M. (1991) *Genes Dev.* **5,** 160–174.
25. Almasan, A., Linke, S. P., Paulson, T. G., Huang, L. & Wahl, G. M. (1995) *Cancer Metastasis Rev.* **14,** 59–73.
26. Shibata, T., Cunningham, R. & Radding, C. (1981) *J. Biol. Chem.* **256,** 7557–7564.
27. Sambrook, J., Fritsch, E. F. & Maniatis, T. (1989) *Molecular Cloning: A Laboratory Manual* (Cold Spring Harbor Lab. Press, Plainview, NY).
28. Jain, S. K., Inman, R. B. & Cox, M. M. (1992) *J. Biol. Chem.* **262,** 4215–4222.
29. La Morte, V. J., Goldsmith, P. K., Spiegel, A. M., Meinkoth, J. L. & Feramisco, J. R. (1992) *J. Biol. Chem.* **267,** 691–694.
30. Linke, S., Clarkin, K., De Leonardo, A., Tso, A. & Wahl, G. M. (1996) *Genes Dev.*, in press.
31. Jones, C. & Wynford-Thomas, D. (1995) *Trends Genet.* **11,** 165–166.
32. Xiao, H., Pearson, A., Coulombe, B., Truant, R., Zhang, S., Regier, J. L., Triezenberg, S. J., Reinberg, D., Flores, O., Ingles, C. J. & Greenblatt, J. (1994) *Mol. Cell. Biol.* **14,** 7013–7024.
33. Yamaizumi, M. & Sugano, T. (1994) *Oncogene* **9,** 2775–2784.
34. Mercer, W. E., Shields, M. T., Amin, M., Sauve, G. J., Appella, E., Romano, J. W. & Ullrich, S. J. (1990) *Proc. Natl. Acad. Sci. USA* **87,** 6166–6170.
35. Swanson, J. A., Lee, M. & Knapp, P. E. (1991) *J. Cell Biol.* **115,** 941–948.
36. Minaschek, G., Bereiter-Hahn, J. & Berthholdt, G. (1989) *Exp. Cell Res.* **183,** 434–442.
37. Capecchi, M. R. (1980) *Cell* **22,** 479–488.
38. Ishizaka, Y., Chernov, M., Burns, C. M. & Stark, G. (1995) *Proc. Natl. Acad. Sci. USA* **92,** 3224–3228.
39. Iliakis, G. (1991) *Bioessays* **13,** 641–648.
40. Frankenberg, S. M. (1990) *Radiat. Environ. Biophys.* **29,** 273–292.
41. Huberman, J. A. & Riggs, A. D. (1968) *J. Mol. Biol.* **32,** 327–341.
42. Kadyk, L. C. & Hartwell, L. H. (1992) *Genetics* **132,** 387–402.
43. Desautels, L., Brouillette, S., Wallenburg, J., Belmaaza, A., Gusew, N., Trudel, P. & Chartrand, P. (1990) *Mol. Cell. Biol.* **10,** 6613–6618.
44. Agarwal, M. L., Agarwal, A., Taylor, W. R. & Stark, G. R. (1995) *Proc. Natl. Acad. Sci. USA* **92,** 8493–8497.
45. Roth, D., Porter, T. & Wilson, J. (1985) *Mol. Cell. Biol.* **5,** 2599–2607.
46. Zetterberg, A. & Larsson, O. (1985) *Proc. Natl. Acad. Sci. USA* **82,** 5365–5369.
47. Greider, C. W. (1990) *Bioessays* **12,** 363–369.
48. Allsopp, R. C., Vaziri, H., Patterson, C., Goldstein, S., Younglai, E. V., Futcher, A. B., Greider, C. W. & Harley, C. B. (1992) *Proc. Natl. Acad. Sci. USA* **89,** 10114–10118.
49. Bennett, C. B., Lewis, A. L., Baldwin, K. K. & Resnick, M. A. (1993) *Proc. Natl. Acad. Sci. USA* **90,** 5613–5617.
50. Sandell, L. L. & Zakian, V. A. (1993) *Cell* **75,** 729–739.
51. Oberosler, P., Hloch, P., Ramsperger, U. & Stahl, H. (1993) *EMBO J.* **12,** 2389–2396.
52. Jayaraman, L. & Prives, C. (1995) *Cell* **81,** 1021–1029.
53. Gottlieb, T. M. & Jackson, S. P. (1993) *Cell* **72,** 131–142.
54. Rathmell W. K. & Chu G. (1994) *Proc. Natl. Acad. Sci. USA* **91,** 7623–7627.
55. Metzger, L. & Iliakis, G. (1991) *Int. J. Radiat. Biol.* **59,** 1325–1339.
56. Wong, E. A. & Capecchi, M. R. (1985) *Somat. Cell Mol. Genet.* **11,** 43–51.
57. Friedberg E. C., Walker G. C. & Siede W. (1995) *DNA Repair and Mutagenesis* (Am. Soc. for Microbiol., Washington), pp. 283–316.